ARTICLE

Alkali Etching of a Poly(lactide) Fiber

Shih-Po Sun,[†] Mei Wei,[‡] James R. Olson,[§] and Montgomery T. Shaw*[,†,‡]

Polymer Program, Institute of Materials Science, and Department of Chemical, Materials and Biomolecular Engineering, University of Connecticut, Storrs, Connecticut 06269-3136, and Teleflex Medical, 1295 Main Street, P.O. Box 219, Coventry, Connecticut 06238

ABSTRACT Alkali etching of a poly(L-lactic acid) fiber was studied by exposing the fiber surface to sodium hydroxide solutions. The factors examined included the etching time (0−1.5 h), alkali concentration (0.25−3 mol/L), and etching temperature (25−80 °C). The extent of etching was determined gravimetrically. Both weight loss and mechanical testing results suggest that alkali etching is strictly a surface hydrolysis reaction, as opposed to a bulk reaction, and thus the weight loss rate decreases with a shrinking fiber radius. A slight increase in the fiber crystallinity observed from thermal analysis was interpreted as a result of surface-limited etching on a sheath−core fiber microstructure. The dependence of the rate on the alkali concentration is nonlinear, suggesting that the fiber weight loss rate is subject to both chemical hydrolysis and transport limitations. The dependence of the rate on the temperature follows the Arrhenius equation. The fiber weight after etching can thus be predicted by an overall expression combining all factors: time, temperature, concentration, and fiber diameter.

KEYWORDS: PLLA fiber • surface etching • etching kinetics • fiber modulus • fiber strength • surface roughening

INTRODUCTION

Because of its biodegradability, poly(L-lactic acid) (PLLA) has already found wide application in biomedical implants (1), tissue engineering scaffolds (2), and drug-releasing materials (3). PLLA is an appropriate biomaterial for longer term implantation and has known good biocompatibility for wound-closure applications. However, for applications where either mineral nucleation or cell attachment and growth are desired, its surface must be made more accommodating by surface modification. Primary methods of surface modification are alkaline etching or copolymerization with more hydrophilic monomers (3). Attempts have been made to increase the hydrophilicity by blending, copolymerizing, coating, and grafting hydrophilic substances (4−8). Surface hydrolysis can also improve the hydrophilicity of PLLA (9). Our goal was to develop practical information about etching of the PLLA fiber under alkaline conditions as a step in its eventual use in preparing components for biocomposites. An etched surface, for example, could improve the stress transfer between the matrix and fiber by a combination of mechanical interlocking, due to increased surface roughness, and chemical bonding. We chose PLLA-spun fibers among all of the possible forms (e.g., film, molded shapes) because fibers with high mechanical strength are appropriate for use in composites, as well in traditional applications such as sutures and braided prostheses (10, 11). Most of the studies of PLLA surface hydrolysis have used film (12−14), as opposed to fiber, and the primary observations have been changes of the morphology and mechanical properties (15−19). Some researchers have examined the hydrolysis mechanism using poly(lactide) (PLA) monolayers (20, 21). However, to develop practical engineering information, we focused on the hydrolysis kinetics of fibers.

Alkaline etching is considered to result from hydrolysis (saponification) of ester linkages along the PLLA chain. This reaction is expected to create terminal carboxylate and hydroxyl groups on the fiber surface. These exposed hydrophilic groups not only make the PLLA fiber surface more hydrophilic, which is important for cell attachment (22), but also provide reactive sites on the fiber that can be exploited to improve the bonding between the fiber and matrix in making composites (23, 24). For example, in a curing polyurethane matrix system, the isocyanate groups can react with both the hydroxyl and carboxyl groups to form a strong bond with the fiber surface. Unlike bulk hydrolysis, which takes place in an acid or simulated body fluid (18, 25), alkaline hydrolysis is thought to be a surface reaction, which changes only the surface properties of the PLLA fiber without seriously affecting its core (3, 17, 26). A reaction that is strictly confined to the surface can lead to the desired surface chemical properties without reducing the mechanical strength of the fiber. While a surface reaction has been indicated by previous studies on the film, fibers have not been examined directly. With a unique morphology, the results with fibers might be quite different from those reported for the film.

We studied the kinetics of hydrolysis by monitoring the weight loss under different etching conditions. A kinetic model for surface hydrolysis on a cylindrical fiber was proposed and compared with the bulk reaction. The variables studied included the etching time and temperature, alkali concentration, and, indirectly, fiber radius. Nonlinear, least-squares modeling was used to derive the parameters

* E-mail: montgomery.shaw@uconn.edu.

Received for review April 3, 2009 and accepted June 17, 2009

[†] Polymer Program, Institute of Materials Science, University of Connecticut.

[‡] Department of Chemical, Materials and Biomolecular Engineering, University of Connecticut.

[§] Teleflex Medical.

DOI: 10.1021/am900227f

Published on Web 07/06/2009

Table 1. Conditions for the Etching of PLLA Fibers

temperature, °C	etching time, min	NaOH concentrations, mol/L
25	10	0.25, 0.5, 2, 3
25	30	0.25, 0.5, 2, 3
25	60	0.25, 0.5, 2, 3
25	90	0.25, 0.5, 2, 3
35	30	0.25, 0.5, 1, 2
40	30	0.25, 0.5, 1, 2
50	30	0.25, 0.5, 1, 2
57	30	0.25, 0.5, 1, 2
65	30	0.25, 0.5, 1, 2
80	30	0.25, 0.5, 1, 2

of the kinetic equations. The influence of the etching time, alkaline concentration, and temperature on the weight loss were derived in sequence through progressive building of a kinetic expression. The final general kinetic expression was fitted to the entire set of relative weight loss data comprising 40 independent observations, yielding several kinetic parameters. These parameters were all significant at the 95% probability level. The residuals were tested for variance uniformity and normality. In addition to weight loss, the effects of alkaline etching on the fiber crystallinity were examined. The mechanical properties of these etched fibers were also measured. While the reported results are confined to one material, the methods and, to some extent, the nature of the dependencies of the etching rate on conditions should translate to other fibers.

EXPERIMENTAL SECTION

Materials. The PLLA fiber used in the current investigation was a melt-spun 30-filament yarn obtained from Teleflex Medical. It was spun from melt-polymerized lactide (a dimer of lactic acid) of the L form and extruded through a 30-hole spinneret. After cooling, the extruded and untwisted 140-denier yarn was then further stretched at 110 °C with a drawing ratio of 4.3:1. The resulting fibers had an average diameter of 23.7 μm, with a sample standard deviation of 1.2 μm. Where needed, an original fiber radius r_0 of 11.85 μm and the theoretical density ρ of 1.2 g/cm^3 were assumed. The weight-average molecular weight was 60.3 kDa, and the polydispersity index was 1.49. Etching solutions were prepared using reagent-grade sodium hydroxide and deionized water from a Millipore Milli-Q system. Their concentrations ranged from 0.25 to 3 mol/L.

Etching Procedure. PLLA yarn samples ranging from 10 to 60 mg were enclosed loosely in a custom-made, 40-mesh stainless steel spherical cage with an inner diameter of 50 mm. This assembly was then immersed in 500 mL of a sodium hydroxide solution. The NaOH-to-fiber weight ratio in the solution was kept higher than 1000 (1600:1 mole ratio) to assure nearly a constant pH during the etching process. Mild mechanical agitation was applied to prevent local concentration buildup. The chosen factor levels for the etching time, sodium hydroxide concentration, and temperature are listed in Table 1. To remove residual sodium hydroxide after hydrolysis, the yarns were repeatedly rinsed in deionized water until the rinse water was neutral. The samples were then vacuum dried for 12 h at room temperature before further characterization. Each test unit was used for only one determination; i.e., the specimens were not returned to the reaction bath for additional etching. Thus, all results were processed as a relative weight, $W(t)/W_0$, where $W(t)$ is the weight of the specimen after etching for time t and W_0 is the initial weight of the specimen. The samples for tensile testing were etched following the same procedure except that the yarn was wrapped on a poly(tetrafluoroethylene) frame for easy retrieval.

Characterization. The weights of vacuum-dried PLLA fiber samples before and after etching were measured to the nearest 10 ng with an analytical balance (Mettler Toledo, model AX105). Images of the fibers were taken by a JEOL 6335F field-emission scanning electron microscope. The fiber diameter was then determined using image analysis software. Three fibers were chosen at random from each run, and five diameters were measured on each fiber. Mechanical properties were evaluated using a tensile tester (Instron, model 3342) equipped with pneumatic yarn grips. The strain rate was kept at 2 min^{-1}. Because fibers break consecutively in a multifilament yarn, a gradual decrease of the load was observed after breakage of the first single fiber. The strength was thus determined as the ultimate stress right before breaking of the first fiber in the yarn. Gel permeation chromatography measurements were conducted on a Waters 410 gel permeation chromatograph with tetrahydrofuran as the eluent (flow rate 1 mL/min, 35 °C). The molecular weights were calibrated against polystyrene standards. The crystallinity of the fiber was determined using a differential scanning calorimeter (TA, model Q20). A 50 K/min heating rate was used to minimize recrystallization of amorphous PLA. Two scans were conducted on each specimen, and only the endothermic melting peak in the first heating scan was used to determine the crystallinity because no discernable crystallization peak during heating was observed.

RESULTS AND DISCUSSION

The weight loss of a hydrolyzed fiber is logically a result of polymer−chain fragments being dissolved as carboxylate by the sodium hydroxide solution. The expected ultimate end product, sodium lactate, would not necessarily be the leaving species because higher oligomers would also undoubtedly be soluble or able to form micelles. Thus, the rate of sodium lactate production would not be a valid indicator of the rate of fiber etching.

Fiber Radius. We can hypothesize that if the hydrolysis reaction between a PLLA ester linkage and hydroxides of a sodium hydroxide solution takes place on the fiber surface, the severed chain will be washed away to expose a fresh surface for further reaction. While retaining its cylindrical shape, the fiber surface will be peeled off layer by layer, causing a gradually diminishing radius. The weight for a cylindrical fiber with a uniform density at time t can thus be expressed as

$$W(t) = W_0\left(\frac{r(t)}{r_0}\right)^2 \quad (1)$$

where $r(t)$ is the radius after etching and r_0 and W_0 are the original fiber radius and weight, respectively. Figure 1 shows the radii of samples with different residual weight fractions from groups in Table 1. It is seen that the observed radii follow eq 1 closely, which is consistent with the premise that the hydrolysis reaction occurs on the fiber surface, even when the weight loss is high (~80%). This agrees with findings for the alkaline hydrolysis of PLLA films, which also follows a surface erosion mechanism (12).

Weight Loss Kinetics and Mechanisms. If the hydrolysis is a surface reaction, then the rate of weight loss

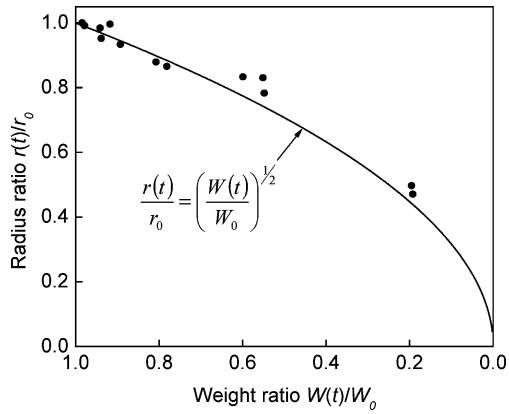

FIGURE 1. Experimental data of the fiber radius at different residual weight fractions compared with a cylindrical fiber model.

should decrease because the fiber surface area diminishes as the reaction proceeds. Two rate models are therefore considered to test this premise: (1) a surface reaction, in which the weight loss rate is proportional to the surface area, and (2) a bulk reaction, in which the weight loss rate is proportional to the fiber volume. The first can be expressed as

$$\frac{dW(t)}{dt} = -kA(t) \tag{2a}$$

where $A(t)$ is the time-dependent surface area. Recognizing that the observations in this study are $W(t)/W_0$, we divide both sides of eq 2a by W_0. Simple geometric considerations show that $W_0/A_0 = \rho r_0/2$, where ρ is the fiber density. Thus, a dimensionally simplified form can be written as

$$\frac{d[W(t)/W_0]}{dt} = -k_{A*}[A(t)/A_0] \tag{2b}$$

where $k_{A*} = k\rho r_0/2$. For a given fiber, either of the two rate constants k and k_{A*} can be used.

Similarly, for the volume-dependent rate, we can write

$$\frac{dW(t)}{dt} = -kV(t) \tag{3a}$$

where $V(t)$ is the time-dependent volume of the sample, and

$$\frac{d[W(t)/W_0]}{dt} = -k_V[V(t)/V_0] \tag{3b}$$

where $k_V = k\rho$. In all cases, the subscript 0 indicates the initial values.

The above equation sets serve then as the basis for examining the premise of surface etching using the kinetics of weight loss alone. They represent the limits of behavior during fiber degradation.

Integration of eqs 2b and 3a using geometrical identities leads to

$$W(t)/W_0 = 1 - 2k_At + (k_At)^2 \quad k_A = 0.5k_{A*},\ t \le 1/k_A \tag{4}$$

for surface control and

$$W(t)/W_0 = e^{-k_Vt} \tag{5}$$

for volume control.

The experiment of fibers etched with 3 M NaOH at 25 °C for up to 450 min was conducted to study the rate-versus-area dependence at a high weight loss ratio (>0.9). The results, along with the models, are shown in Figure 2. A model invoking a constant rate of weight loss is also shown for comparison as a dashed line. It is seen that the data follow closely the trend predicted by the surface reaction model (eq 2a). There is, however, a mild discrepancy toward a higher weight loss rate at later stages of etching. This may be due to the roughening of the fiber surface, which can be seen in the micrograph displayed in Figure 3. The roughening, along with pits and cracks, results in a larger surface area than that for a a smooth fiber with the same radius (27). This excess surface area compensates for the decreasing surface area caused by a shrinking fiber radius and keeps the weight loss rate from dropping. The volume-dependent rate expression (eq 5) is not describing the trend in the data correctly.

Effects of the Concentration and Temperature. Knowing that the fiber etching is a surface reaction, the area-dependent, weight loss expression (eq 4) was chosen for examination of the influence of the alkali concentration and temperature. The relative weights of fibers etched in an alkali solution with different concentrations are shown in Figure 4. The rate constant k_A was derived from a fitting of these data with eq 4. The effects of the concentration and temperature on k_A are depicted in Figures 5 and 6, respectively.

We now seek to find the functional form of the C and T dependencies. The trends in Figure 5 suggest a nonlinear dependence of k_A with respect to the concentration, e.g.,

$$k_A = b + aC^n \tag{6}$$

where C is the sodium hydroxide concentration in mol/L and a and b are constants dependent only on the temperature. The extrapolated values for k_A at zero concentration (Figure 5), b, are not zero, suggesting incorrectly that pure water causes etching. A possible explanation for this is a very rapid etching of a susceptible surface layer or removal of surface contaminants, e.g., dust particles, or a spin lube that takes place almost immediately upon immersion of the fibers in caustic. It was observed, as expected, that both a and b increased with the temperature. Attempts to fit the weight-loss data with zero-intercept expressions led to unsatisfactory descriptions of the early part of the etching process.

Figure 6 shows the dependence of k_A on the etching temperature. The trends suggest an Arrhenius relationship

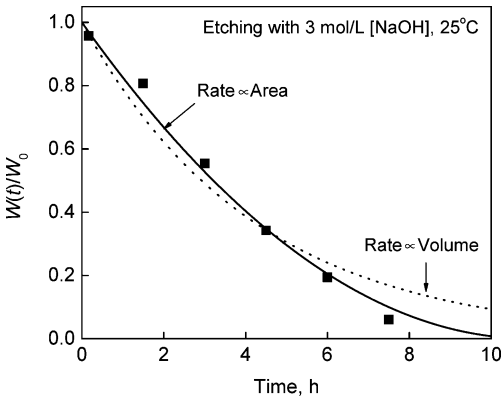

FIGURE 2. Comparison of fibers subjected to 3 M NaOH at 25 °C with predictions of area-dependent, volume-dependent, and constant rates.

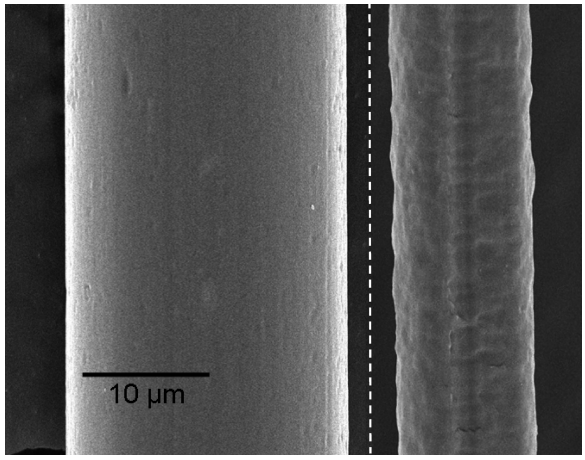

FIGURE 3. Scanning electron microscopy image of the fiber surface after 6 h in 3 mol/L NaOH at 25 °C (right) compared with the fiber before etching (left).

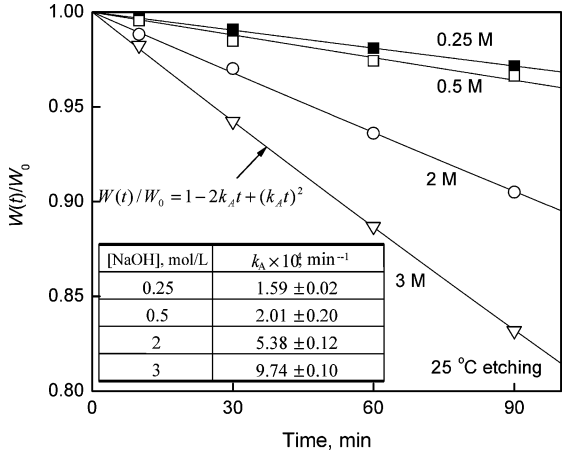

FIGURE 4. Dependence of the fiber weight ratio on the etching time at 25 °C.

of k_A with respect to the temperature. We can now express $k_A(C,T)$ as

$$k_A = A_a e^{-E_a/RT}\left(\frac{C}{C_0}\right)^n + A_b e^{-E_b/RT} \qquad (7)$$

Following the Arrhenius equation, the temperature-dependent constants a and b are now expressed in the form

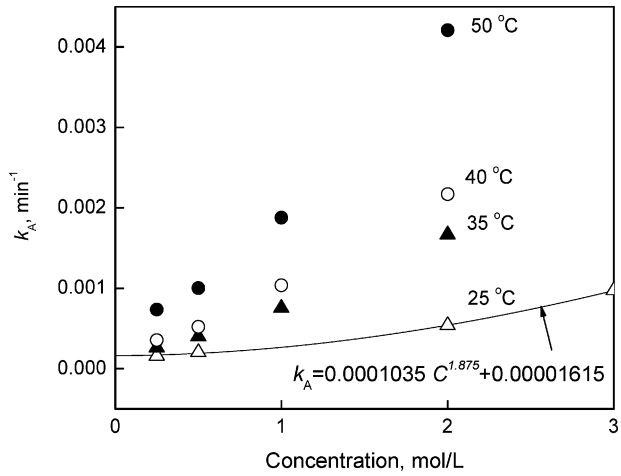

FIGURE 5. Dependence of k_A on the NaOH concentration at 25, 35, 40, and 50 °C. A sample fit to eq 6 is shown for the 25 °C data.

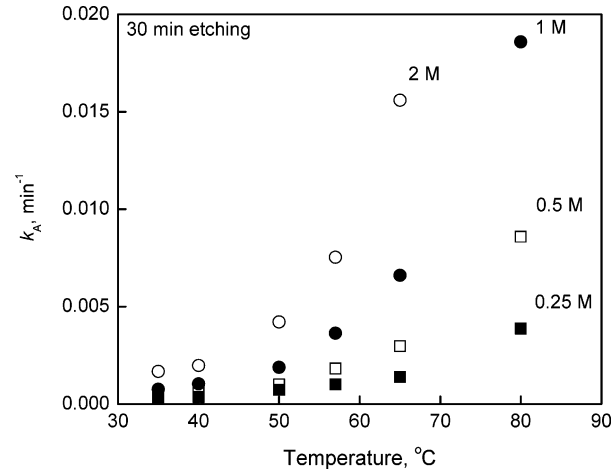

FIGURE 6. Dependence of k_A on the etching temperature with [NaOH] of 0.25, 0.5, 1, and 2 mol/L.

Table 2. Values of the Parameters in Equation 7

parameter	value[a]
A_a	$2.7 \times 10^9 \pm 1.0 \times 10^9$
E_a, kJ/mol	75.6 ± 1.2
N	1.4 ± 0.03
A_b	68.9 ± 103.9
E_b, kJ/mol	32.0 ± 4.2

[a] The ± are 95% confidence intervals.

of $a(T) = A_a \exp(-E_a/RT)$ and $b(T) = A_b \exp(-E_b/RT)$ where A_a and A_b are frequency factors for a and b, respectively. E_a and E_b are activation energies for a and b, respectively. A reduced concentration C/C_0, where $C_0 = 1$ mol/L, is introduced to keep the overall expression dimensionless. The parameters derived from fittings of the results of all treatment conditions in Table 1 are listed in Table 2. The activation energy for constant a is $E_a = 76$ kJ/mol, which is similar to the activation energy of 75−84 kJ/mol when PLLA is hydrolyzed in a phosphate-buffered solution (pH ∼ 7.4) (28). The activation energy for constant b is $E_b = 32$ kJ/mol. These different activation energies for constants a and b make k_A not simply factorable into concentration and temperature terms.

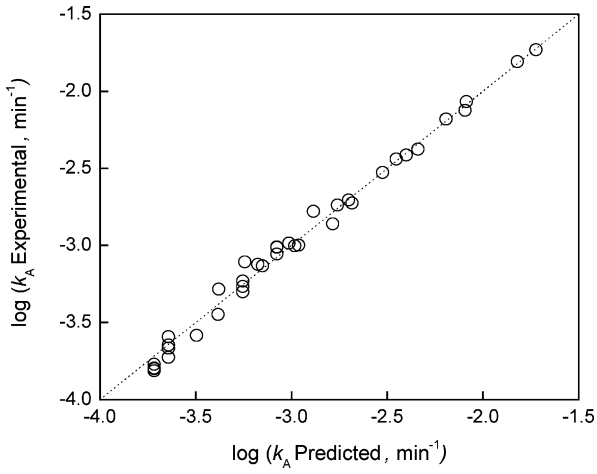

FIGURE 7. Comparison of the experimental fractional weight loss and those predicted by eq 7.

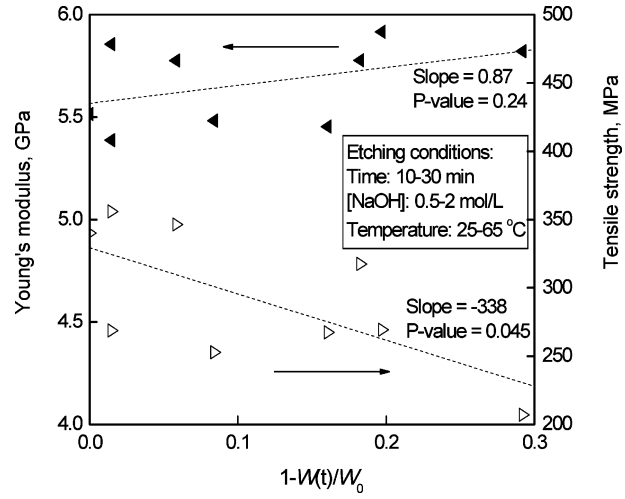

FIGURE 8. Mechanical properties of fibers with different weight loss ratios.

Figure 7 shows the validity of this general expression. The predicted and experimental k_A values for all of the treatment conditions listed in Table 1 fall satisfactorily along the slope = 1 line, demonstrating the validity of eq 7. The residuals of the experimental rate constants passed the usual tests for normality and uniform variance, suggesting the independence of our observations. One can use eq 7 to decide etching conditions to reach the desired weight loss. To reach a 10% weight loss within 30 min, for example, a k_A value of 0.00171 calculated from eq 4 is required. If the etching is conducted at 35 °C, a NaOH concentration of $C = 2.43$ mol/L is thus needed, judging from eq 7. For a PLLA fiber of different diameter, the estimated value of k_A will need to be scaled with a ratio of the desired fiber radius r_{new} to the radius of the fiber used in this experiment. Thus

$$k_{A,\text{new}} = k_{A,11.85\mu\text{m}} \frac{r_{\text{new}}}{11.85\,\mu\text{m}} \tag{8}$$

Over the range of etching conditions used in this study, it can be seen that a higher weight loss rate can be achieved more readily by increasing the temperature rather than the concentration. For example, it is more practical to achieve a 10-fold weight loss rate by increasing the temperature by 20 °C than by increasing the alkali concentration by a factor of 6. This agrees with other findings involving the etching of poly(ethylene terephthalate) fibers or fabrics with alkali solutions (29−34). A drawback of elevated temperature is that warming close to $T_g = 55$ °C of PLLA might be expected to result in unwanted chain rearrangement and secondary crystallization, resulting in the loss of mechanical properties; however, the results indicated that this was not a problem.

The higher-than-first-order dependence of the weight loss rate on the hydroxide ion concentration, n, in Table 2 is not in accordance with the first-order rate implied by the hydrolysis reaction mechanism, which requires only one hydroxide ion for ester bond cleavage. This discrepancy toward a higher weight loss rate with increasing hydroxide ion concentration is perhaps more physical in nature than chemical, i.e., is a result of the concentration dependence of the interaction of the hydrolytic medium with the polymer. Because of the hydrophobic nature of the unhydrolyzed fiber, the entire fiber surface is not readily covered by the alkali solution, especially in view of the geometry of the fiber bundle and the possibility of trapped air. Accordingly, increasing the hydroxide concentration lowers the surface tension of the fluid, which aids in wetting of the fiber surface to create more available surface for reaction. Combined with a first-order hydrolysis reaction, the increase of the available fiber surface makes the overall weight loss rate depend on the alkali concentration to a power higher than 1. Although similar kinetics have also been observed by others, e.g., Ginde et al. (35), there has been little in the way of an explanation for the phenomenon. While the hypothesis of concentration-dependent wetting seems reasonable, there are certainly other possibilities, including the removal of larger polymer fragments at higher concentrations, a possible source of the pits observed on the fiber surface.

To test the proposed wetting hypothesis, the reaction order should be checked under conditions that provide intense mixing between the fibers and the reagent. In addition, a preliminary wash with a surfactant might also be useful for making sure that all fiber surfaces are completely wetted.

Assuming that the properties of the fiber are spatially uniform, the mechanical properties of the alkali-etched PLA fibers should not deteriorate if the etching takes place merely on the fiber surface and leaves the inner core unaffected. Selected samples covering different weight losses are compared in Figure 8. No significant linear correlation between the modulus and weight loss can be deduced from the observations ($P = 0.24$). The strength, on the other hand, decreases with an increase in the weight loss ($P = 0.045 < 0.05$). This is reasonable in view of the pits and cracks created (Figure 3) because these defects can act as initiation sites for crack formation, leading to fiber breakage (32). The loss in the tensile strength may be quite acceptable in composites where the strength requirements are modest or where modulus enhancement is the primary goal.

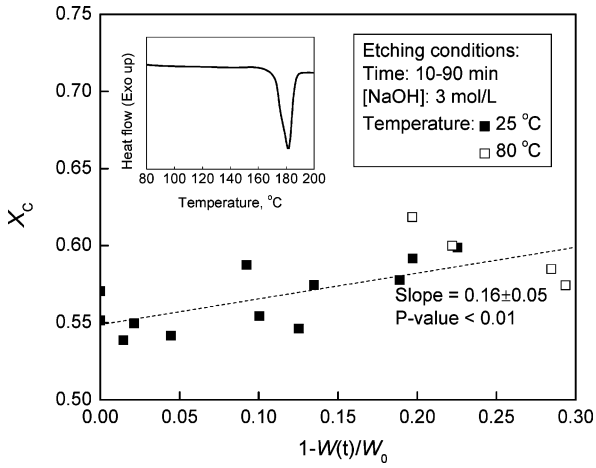

FIGURE 9. Changes in the crystallinity of an etched PLA fiber at different weight loss ratios.

Thermal analysis of etched PLLA fibers also reveals the effects of etching on the fiber microstructure or, alternatively, changes of crystallinity with the radius. An example of the first heating cycle of an etched PLLA fiber from differential scanning calorimetry (DSC) measurements is shown near the top of Figure 9. There are no discernable secondary crystallization peaks, which can usually be found around 100 and 165 °C (36, 37). Thus, crystallization induced by heating during scanning is eliminated, and the crystallinity fraction of the fiber, X_c, can be derived from only the heat of fusion, ΔH_f, of the melting peak at 180 °C without a correction for crystallization (eq 9).

$$X_c = \frac{\Delta H_f}{\Delta H_f^\circ} \tag{9}$$

The heat of fusion of 100% crystallinity PLLA, ΔH_f°, in eq 9 is 93 J/mol (38). The resulting crystallinities at different weight loss ratios up to 30% weight loss ratio are shown in Figure 9. A slight, but highly significant, increase of the crystallinity is observed. The trend predicts a 3% increase of crystallinity when achieving 30% weight loss. As the etching proceeds toward the core of the fiber, either an increase or a decrease of the crystallinity of the remaining fiber has been observed by others with alkali-etched PET fibers (33, 39). It was reported that polymer chains near the surface of a rapidly spun (>1615 m/min) PET move more freely when leaving the spinneret, and this may result in a more oriented and crystallized surface layer during cooling. The PET fibers spun at lower speeds show opposite results, but no explanations have been provided. The fibers used in our study also have a low linear spinning speed of about 300 m/min. Because the fibers are relatively thick, the inside may have slightly more time to crystallize, resulting in higher values of X_c. In addition, there will be a hydrostatic tension inside the cooling fiber, which could extend the crystallization time.

Except for the inherent possible radial variation of the microstructure, the annealing effect on fibers treated at elevated temperatures could also contribute to an increase of the crystallinity as the etching proceeds. By exposure of fibers to 80 °C deionized water for 30 min, which is the highest treatment temperature and longest treatment time in our study, an endotherm around 90−100 °C should exist if annealing occurred. Because no endotherm was observed, the annealing effect can probably be eliminated. The selective removal of amorphous regions in the fiber may lead to this increase of crystallinity as well. However, this change, according to the surface-etching hypothesis, will be confined to the thin surface layer and thus would not show up well in the DSC scans. The surface-limited swelling in the amorphous region may also lead to an increase of crystallinity with etching (25). The mobility of the swollen amorphous chain during scission will increase significantly, resulting in a crystalline structure after drying (40). This resembles the well-known solvent-induced crystallization. Indeed, a slight increase of the fiber crystallinity has also been observed when PGA fibers are subjected to alkaline etching (35). Although statistically significant, the variation of crystallinity with the radius is judged to be insufficient to have an impact on the etching kinetics.

CONCLUSIONS

We learned that the etching time, alkali concentration, and etching temperature all affect the weight loss of a PLLA fiber differently. An attempt has also been made to correlate these factors with fiber weight loss, which can be used to design etching conditions to reach the desired fiber radius. The results are consistent with surface area control of the etching rate, which, along with the tensile testing results and thermal analysis, suggests that alkaline etching is a surface reaction. Thus, moderate alkaline etching should be able to increase the hydrophilicity of the PLLA fiber surface without greatly affecting the fiber's mechanical or thermal properties.

While the results reported here are confined to one fiber, the manufacturers of high-strength PLLA fibers tend to use PLLA of very high isomeric purity and high molecular weight to gain the best properties. Thus, it is reasonable to suggest that the kinetic expressions will apply to other PLLA fibers that are manufactured using a similar spinning and drawing sequence. At the very least, the reported effects of temperature and concentration on the etching rates should provide reasonable relative estimates for other fibers.

Acknowledgment. The authors acknowledge financial support from NSF GOALI Grant BES-0503315, Connecticut Innovations under the Yankee Ingenuity Technology Competition, and Taiwan Merit Scholarship 0941A022.

APPENDIX

Nomenclature

$A(t)$	fiber surface area
C	alkali concentration
E	activation energy
ΔH_f	heat of fusion
k_A	area-dependent rate constant
k_v	volume-dependent rate constant
R	gas constant

$r(t)$	fiber radius
r_0	fiber radius before etching
T	etching temperature
t	etching time
$W(t)$	fiber weight
W_0	fiber weight before etching
X_c	crystallinity

DERIVATION OF EQS 5 AND 6.

$$\frac{\mathrm{d}[W/W_0]}{\mathrm{d}t} = -k_{A^*}[A/A_0]$$

$$\frac{\mathrm{d}W}{\mathrm{d}t} = -k_{A^*}W_0\left(\frac{W}{W_0}\right)^{1/2}$$

$$W^{-1/2}\,\mathrm{d}W = -k_{A^*}{W_0}^{1/2}\,\mathrm{d}t$$

$$\int_{W_0}^{W} W^{-1/2}\,\mathrm{d}W = \int_0^T -k_{A^*}{W_0}^{1/2}\,\mathrm{d}t$$

$$2W^{1/2}\big|_{W_0}^{W} = -k_{A*}{W_0}^{1/2}t\big|_0^T$$

$$2(W^{1/2} - W_0^{1/2}) = -k_{A^*}{W_0}^{1/2}(T - 0)$$

$$2W^{1/2} = -k_{A^*}{W_0}^{1/2}T + 2{W_0}^{1/2}$$

$$2W^{1/2} = {W_0}^{1/2}(-k_{A^*}T + 2)$$

$$\left(\frac{W}{W_0}\right)^{1/2} = 1 - \frac{1}{2}k_{A^*}T$$

$$\left(\frac{W}{W_0}\right) = \left(1 - \frac{1}{2}k_{A*}T\right)^2$$

$$\frac{W}{W_0} = 1 - k_{A^*}t + \left(\frac{1}{2}k_{A*}t\right)^2$$

$$\frac{W}{W_0} = 1 - 2k_At + (k_At)^2, \quad k_A = 0.5k_{A^*}$$

$$\frac{\mathrm{d}[W/W_0]}{\mathrm{d}t} = -k_V[V/V_0]$$

$$\frac{1}{W_0}\frac{\mathrm{d}W}{\mathrm{d}t} = -k_V\left(\frac{W}{W_0}\right)$$

$$\frac{1}{W}\,\mathrm{d}W = -k_V\,\mathrm{d}t$$

$$\int_{W_0}^{W}\frac{1}{W}\,\mathrm{d}W = \int_0^T -k_V\,\mathrm{d}t$$

$$\ln W\big|_{W_0}^{W} = -k_Vt\big|_0^T$$

$$\ln W - \ln W_0 = -k_VT$$

$$W/W_0 = \mathrm{e}^{-k_Vt}$$

REFERENCES AND NOTES

(1) Matsusue, Y.; Nakamura, T.; Iida, H.; Shimizu, K. *J. Long-Term Eff. Med. Implants* **1997**, *7*, 119–137.
(2) Freed, L. E.; Marquis, J. C.; Nohria, A.; Emmanual, J.; Mikos, A. G.; Langer, R. *J. Biomed. Mater. Res.* **1993**, *27*, 11–23.
(3) Ha, C.-S.; Gardella, J. A., Jr. *Chem. Rev.* **2005**, *105*, 4205–4232.
(4) Otsuka, H.; Nagasaki, Y.; Kataoka, K. *Sci. Technol. Adv. Mater.* **2000**, *1*, 21–29.
(5) Ma, Z.; Gao, C.; Yuan, J.; Ji, J.; Gong, Y.; Shen, J. *J. Appl. Polym. Sci.* **2002**, *85*, 2163–2171.
(6) Edlund, U.; Kallrot, M.; Albertsson, A.-C. *J. Am. Chem Soc* **2005**, *127*, 8865–8871.
(7) Bhattarai, S. R.; Bhattarai, N.; Viswanathamurthi, P.; Yi, H. K.; Hwang, P. H.; Kim, H. Y. *J. Biomed. Mater. Res., Part A* **2006**, *78*, 247–257.
(8) Boxberg, Y.; Schnabelrauch, M.; Vogt, S.; Salmeron Sanchez, M.; Gallego Ferrer, G.; Monleon Pradas, M.; Suay Anton, J. *J. Polym. Sci., Part B: Polym. Phys.* **2006**, *44*, 656–664.
(9) Yang, J.; Wan, Y.; Tu, C.; Cai, Q.; Bei, J.; Wang, S. *Polym. Int.* **2003**, *52*, 1892–1899.
(10) Agrawal, A. K.; Bhalla, R. *J. Macromol. Sci., Polym. Rev.* **2003**, *43*, 479–503.
(11) Gupta, B.; Revagade, N.; Hilborn, J. *Prog. Polym. Sci.* **2007**, *32*, 455–482.
(12) Tsuji, H.; Ikada, Y. *J. Polym. Sci., Polym. Chem.* **1998**, *36*, 59–66.
(13) Li, S. *J. Biomed. Mater. Res.* **1999**, *48*, 342–353.
(14) Tsuji, H.; Ishida, T. *J. Appl. Polym. Sci.* **2003**, *87*, 1628–1633.
(15) Cam, D.; Hyon, S. H.; Ikada, Y. *Biomaterials* **1995**, *16*, 833–843.
(16) Hyon, S.-H. *Sen'i Gakkaishi* **1998**, *54*, 527–531.
(17) Ma, Z.; Gao, C.; Yuan, J.; Ji, J.; Gong, Y.; Shen, J. *J. Appl. Polym. Sci.* **2002**, *85*, 2163–2171.
(18) Yuan, X.; Mak, A. F. T.; Yao, K. *Polym. Degrad. Stab.* **2002**, *75*, 45–53.
(19) Nishihara, M.; Murase, S. *Sen'i Gakkaishi* **2003**, *59*, 371–374.
(20) Ivanova, T.; Panaiotov, I.; Boury, F.; Proust, J. E.; Benoit, J. P.; Verger, R. *Colloids Surf., B* **1997**, *8*, 217–225.
(21) Lee, W. K.; Gardella, J. A., Jr. *Langmuir* **2000**, *16*, 3401–3406.
(22) Gao, J.; Niklason, L.; Langer, R. *J. Biomed. Mater. Res.* **1998**, *42*, 417–424.
(23) Slivka, M. A.; Chu, C. C.; Adisaputro, I. A. *J. Biomed. Mater. Res.* **1997**, *36*, 469–477.
(24) Mathieua, L. M.; Mueller, T. L.; Bourbana, P.-E.; Pioletti, D. P.; Mullerb, R.; Manson, J.-A. *Biomaterials* **2006**, *27*, 905–916.
(25) Burkersroda, F. V.; Schedl, L.; Göpferich, A. *Biomaterials* **2002**, *23*, 4221–4231.
(26) Wang, S.; Cui, W.; Bei, J. *Anal. Bioanal. Chem.* **2005**, *3*, 547–556.
(27) Holmes, S. A.; Zeronian, S. H. *J. Appl. Polym. Sci.* **1995**, *55*, 1573–1581.
(28) Tsuji, H.; Ikarashi, K. *Biomacromolecules* **2004**, *5*, 1021–1028.
(29) Houser, K. D. *Text. Chem. Color.* **1983**, *15*, 70–72.
(30) Dave, J.; Kumar, R.; Srivastava, H. C. *J. Appl. Polym. Sci.* **1987**, *33*, 455–477.
(31) Zeronian, S. H.; Collins, M. J. *Text. Chem. Color.* **1988**, *20*, 25–28.
(32) Collins, M. J.; Zeronian, S. H. *Text. Prog.* **1989**, *20*, 1–4.
(33) Collins, M. J.; Zeronian, S. H.; Semmelmeyer, M. *J. Appl. Polym. Sci.* **1991**, *42*, 2149–2162.
(34) Kish, M. H.; Nouri, M. *J. Appl. Polym. Sci.* **1999**, *72*, 631–637.
(35) Ginde, R. M.; Gupta, R. K. *J. Appl. Polym. Sci.* **1987**, *33*, 2431–2429.
(36) Zhou, H.; Green, T. B.; Joo, Y. L. *Polymer* **2006**, *47*, 7497–7505.
(37) Di Lorenzo, M. L. *J. Appl. Polym. Sci.* **2006**, *100*, 3145–3151.
(38) Migliaresi, C.; Cohn, D.; De Lollis, A.; Fambri, L. *J. Appl. Polym. Sci.* **1991**, *43*, 83–95.
(39) Holmes, S. A.; Zeronian, S. H. *J. Macromol. Sci., Part A: Pure Appl. Chem.* **1994**, *31*, 1147–1168.
(40) Bajgai, M. P.; Kim, K. W.; Chandra Parajuli, D.; Yoo, Y. C.; Kim, W. D.; Khil, M. S.; Kim, H. Y. *Polym. Degrad. Stab.* **2008**, *93*, 2172–2179.

AM900227F